INSTITUTE OF PHYSICS PUBLISHING SMART MATERIALS AND STRUCTURES
Smart Mater. Struct. **11** (2002) 1–8 PII: S0964-1726(02)32066-4

Resonant controllers for smart structures

H R Pota[1], S O Reza Moheimani[2] and Matthew Smith[3]

[1] School of Electrical Engineering, University College, The University of New South Wales, ADFA Canberra, ACT 2600, Australia
[2] Department of Electrical and Computer Engineering, The University of Newcastle, NSW 2308, Australia
[3] Department of Systems Engineering, RSISE, The Australian National University, ACT 0200, Australia

E-mail: h-pota@adfa.edu.au, reza@ee.newcastle.edu.au and matthew.smith@sysyeng.anu.edu.au

Received 21 March 2000, in final form 29 November 2001
Published 6 February 2002
Online at stacks.iop.org/SMS/11/1

Abstract
In this paper we propose a special type of colocated feedback controller for smart structures. The controller is a parallel combination of high-Q resonant circuits. Each of the resonant circuits is tuned to a pole (or the resonant frequency) of the smart structure. It is proven that the parallel combination of resonant controllers is stable with an infinite gain margin. Only one set of actuator–sensor can damp multiple resonant modes with the resonant controllers. Experimental results are presented to show the robustness of the proposed controller in damping multimode resonances.

1. Introduction

The advancement in materials technology has enabled multi-layered structures where actuators, sensors and the main structure form one whole component [1]. These composite structures are called intelligent or smart structures. Smart structures have found wide applications in areas such as acoustic noise control [2, 3] and vibration control of washing machines [4]. In this paper we propose a controller which is robust and can be programmed to damp only a few or several resonant modes at a time [5]. These controllers have also found application in active noise control of acoustic ducts [6]. The motivation behind this controller is that, in many situations, it may be desirable to embed many discrete actuators in a structure [7] rather than spread out film-type actuators [2]. A necessary requirement for multiple discrete sensor–actuator pairs is that they provide a robust control. The closed-loop robust stability of the controllers suggested in this paper is proven and experimentally demonstrated.

In order to achieve a given task with minimum energy requirements or where large structures are necessary, for example, space structures [7], large telescopes [8] or large antennae, smart structures have an in-built flexibility. The flexibility in the structures is characterized by several resonant modes seen in figure 1 for a cantilever beam. The frequency response in figure 1 is characteristic of most flexible structures; it is the colocated response of a typical flexible structure shown in figure 2.

Due to the resonant modes of flexible structures, a disturbance ($f(d, t)$ in figure 2) results in a response which is highly underdamped and if uncontrolled takes a long time to settle. This undamped response makes the use of an uncontrolled flexible structure unacceptable in most applications. The modelling and control of flexible structures has been a subject of active research for some time now [9–11]. There are several methods to control flexible structures. Under most conditions the disturbance control problem for flexible structures is a linear control problem. It is generally known that colocated velocity feedback results in a robust system with guaranteed closed-loop stability [12, 13]. The stability guarantee is not valid for dynamic actuators. Another equally simple control scheme, known as positive position feedback, has been proposed [14, 15] which retains the guaranteed stability margins. The positive position feedback consists of second-order filters (with no zeros) and the control design consists in suitably choosing the poles and the damping of the filters. The selection of the poles and damping is a non-trivial task and new methods are being proposed [16] to improve the design process. The controllers proposed in this paper are also second-order filters but with two zeros: one zero is at the origin and the other is an LHP real zero. Moreover, the real zero and the complex poles are parameterized by three common parameters which leads to a guaranteed infinite gain stability margin. In addition to these practically attractive qualities, this method can damp multiple modes with only one sensor–actuator pair.

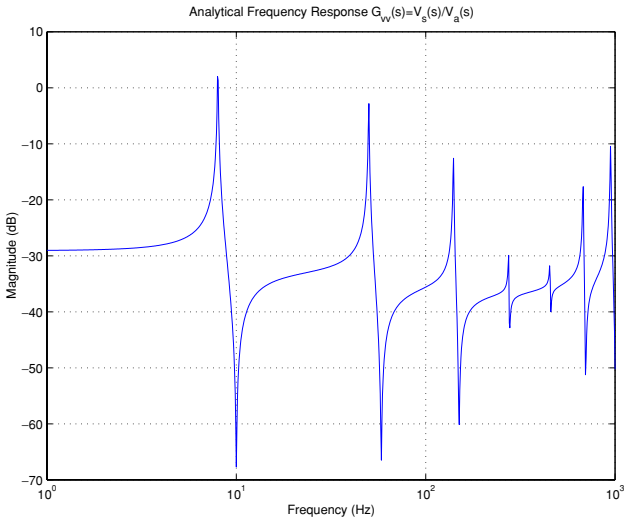

Figure 1. Analytical frequency response.

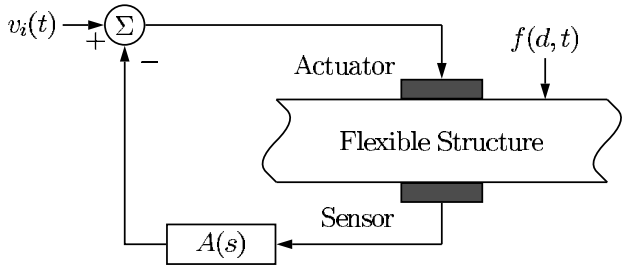

Figure 2. A flexible structure.

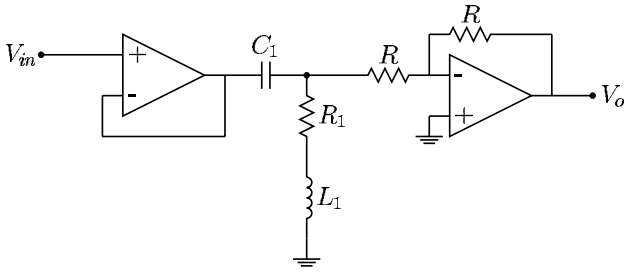

Figure 3. Feedback control RLC network.

Advanced linear control system ideas have also been applied to flexible structures and often with good results. The standard LQG [17], the H^∞ control [18, 19] and minimax LQG [20] have also been successfully used to control flexible structures. The effect of these controllers is to 'push' the resonant peak down, i.e. to increase the system damping. Independent modal control (pp 161–3 in [9]) is another method to damp flexible structures. For effective modal control one actuator per resonant mode is needed. The controller proposed in this paper uses only *one* actuator to damp several of the resonant modes. In this paper 'sensors' and 'actuators' both refer to piezoelectric materials but the proposed method will work for any pair of appropriate sensors and actuators. In short this paper proposes a direct method to 'push' down the resonant peaks using high-Q resonant circuits as shown in figure 3. The results of the experimental validation of this method are presented in this paper.

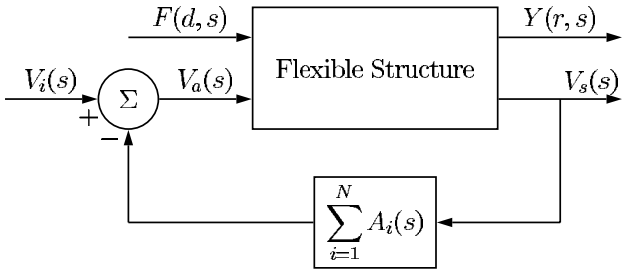

Figure 4. Flexible structure with feedback controller.

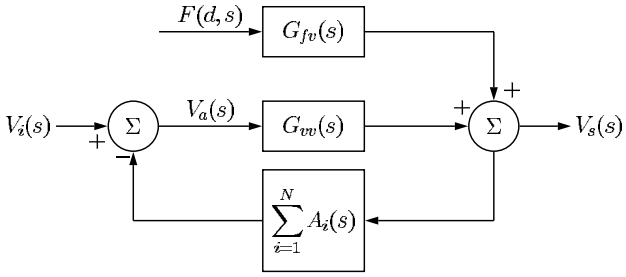

Figure 5. Feedback control block diagram.

This paper is organized as follows. Section 2 discusses the resonant controllers. Section 3 develops the mathematical model of the system. Section 4 proves the closed-loop stability with colocated resonant controllers. Experimental results are presented in section 5 followed by the conclusions.

2. Controller selection and design

The structure of the closed-loop system is shown in figure 4. The disturbance signal is $F(d, s)$, the output sensor voltage is $V_s(s)$, the actuator voltage is $V_a(s)$ and $Y(r, s)$ is the displacement of the structure at location r.

The actuator voltage $V_a(s)$ is given by

$$V_a(s) = -A(s)V_s(s) + V_i(s) \tag{1}$$

where $A(s) = \sum_{i=1}^{N} A_i(s)$ and $A_i(s)$ are of the form

$$A_i(s) = -k_{ai}\frac{C_i s(R_i + L_i s)}{L_i C_i s^2 + R_i C_i s + 1} \tag{2}$$

with $\omega_i^2 = \frac{1}{L_i C_i}$; ω_i is the ith resonant frequency of the flexible structure. The resistance R_i is chosen to maximize the damping of the closed-loop system.

This configuration is motivated by the passive RL network controllers in [21, 22]. In cases where the gain $k_{ai} = 1$, the controller $A_i(s)$ can be completely implemented using a series RLC network shown in figure 3.

Let the block transfer functions in figure 4 be defined as follows for an open-loop situation ($A(s) = 0$):

$$G_{fv}(s) \triangleq \left.\frac{V_s(s)}{F(d,s)}\right|_{V_i(s)=0} \qquad G_{vv}(s) \triangleq \left.\frac{V_s(s)}{V_a(s)}\right|_{F(d,s)=0}$$
$$G_{fy}(r,s) \triangleq \left.\frac{Y(r,s)}{F(d,s)}\right|_{V_i(s)=0} \qquad G_{vy}(r,s) \triangleq \left.\frac{Y(r,s)}{V_a(s)}\right|_{F(d,s)=0}.$$

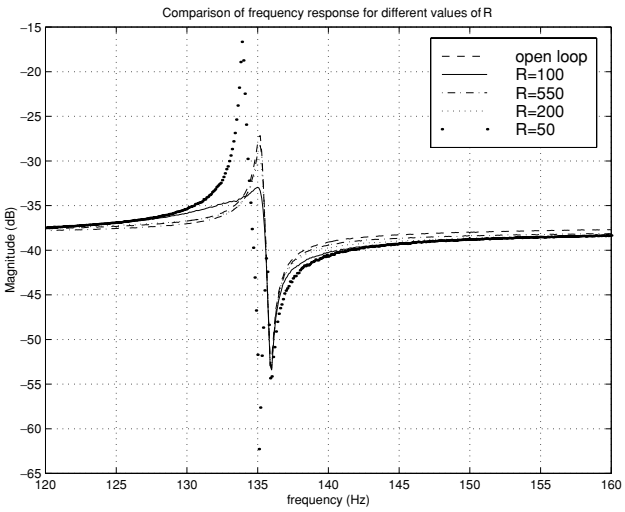

Figure 6. Experimental frequency response for different resistors.

With the above definitions the sensor voltage is given by

$$V_s(s) = G_{fv}(s)F(d,s) + G_{vv}(s)V_a(s).$$

After substituting equation (1) into the above expression

$$V_s(s) = G_{fv}(s)F(d,s) - G_{vv}(s)A(s)V_s(s) + G_{vv}(s)V_i(s)$$

on rearranging the terms the closed-loop transfer function is

$$V_s(s) = \frac{G_{fv}(s)F(d,s)}{1 + A(s)G_{vv}(s)} + \frac{G_{vv}(s)V_i(s)}{1 + A(s)G_{vv}(s)}. \tag{3}$$

Equation (3) can also be used to get displacement at a given location r in the flexible structure

$$Y(r,s) = \frac{G_{fy}(r,s)F(d,s)}{1 + A(s)G_{vv}(s)} + \frac{G_{vy}(r,s)V_i(s)}{1 + A(s)G_{vv}(s)}. \tag{4}$$

From the transfer functions in equations (3) and (4) it can be seen that the feedback is effective only for the frequency range where $|A(\jmath\omega)G_{vv}(\jmath\omega)|$ is large. In the present approach $A(s)$ is a parallel connection of high-Q resonant circuits. Each circuit is tuned to a resonant mode of the flexible structure, making the feedback effective only at resonant frequencies.

2.1. Selection of R

For each resonant controller of equation (2), the values of the inductor and the capacitor are chosen such that the circuit resonant frequency is the same as one of the flexible structure resonant frequencies. The selection of a suitable value of the resistance is the key to obtaining a good closed-loop response. If the damping resistor in the resonant filter of equation (2) is selected to be too low, there is a notch at the resonant frequency and there is an undesirable shift in closed-loop poles. For high values of the resistance there is hardly any damping in the structure. These two effects are shown for an experimental cantilever beam in figure 6. In this study R was chosen from numerical simulations and then experimental observations. The experimental results show the success of this method. Work is under progress to develop a suitable optimality criterion to choose R which is solvable by standard optimization methods.

2.2. Multiple resonant mode controllers

The resonant mode circuit idea can be easily extended to damp multiple resonant modes. Instead of one feedback circuit $A(s)$, several of these circuits can be applied in parallel to give the closed-loop transfer function given below:

$$Y(r,s) = \frac{G_{fy}(r,s)F(d,s)}{1 + \sum_{i=1}^{N} A_i(s)\,G_{vv}(s)} + \frac{G_{vy}(r,s)V_i(s)}{1 + \sum_{i=1}^{N} A_i(s)\,G_{vv}(s)} \tag{5}$$

where the resonant mode filters $A_i(s)$ are of the form given in equation (2). Each resonant filter is tuned to a resonant frequency of the structure. The damping resistor for each of the resonant filters can be chosen independently because the action of the resonant filters is mostly uncoupled. In the next section a cantilever beam is selected to demonstrate these concepts.

3. Model of the laminate beam

We consider the piezoelectric laminate cantilevered beam of figure 7. The beam is fixed at one end and free at the other. The two piezoelectric patches in figure 7 are used as actuators and/or sensors. There are several different approaches to obtain the system model from the solution of the Euler–Bernoulli partial differential equation, with the associated boundary conditions, see for example [23, 24]. However, to find a solution which suits our controller design methodology, we adopt the *assumed modes* approach of [11].

Let $y(r,t)$ denote the elastic deformation of the beam as measured from the rest position. The elastic deflection $y(r,t)$ is governed by the classical Bernoulli–Euler beam equation

$$\frac{\partial^2}{\partial r^2}\left[EI\frac{\partial^2 y(r,t)}{\partial r^2}\right] + \rho A\frac{\partial^2 y(r,t)}{\partial t^2} = C_a\frac{\partial^2 v_a(x,t)}{\partial r^2} \tag{6}$$

where E, I, A, $w(r,t)$ and ρ represent Young's modulus, the moment of inertia, the cross-section area, the external force per unit length and the linear mass density of the beam, respectively. The cantilever beam boundary conditions are

$$\begin{aligned} y(0,t) &= 0 \qquad & EI\frac{\partial y(0,t)}{\partial r} &= 0 \\ EI\frac{\partial^2 y(l,t)}{\partial r^2} &= 0 \qquad & EI\frac{\partial^3 y(l,t)}{\partial r^3} &= 0. \end{aligned} \tag{7}$$

The main idea of the assumed modes approach is to expand the function $y(r,t)$ as an infinite series in the form [11, 25]

$$y(r,t) = \sum_{i=1}^{\infty} q_i(t)\phi_i(r) \tag{8}$$

where $\phi_i(r)$ are the eigenfunctions satisfying the ordinary differential equations, resulting from the substitution of equation (8) into equations (6) and (7). The general form of the mode shapes $\phi_i(r)$ chosen for the beam-type of problem is

$$\phi_i(r) = A_i \sin\lambda_i r + B_i \cos\lambda_i r + C_i \sinh\lambda_i r + D_i \cosh\lambda_i r.$$

There is a considerable latitude in choosing the constants A_i, B_i, C_i and D_i. To fix these constants the mode shapes $\phi_i(r)$ are

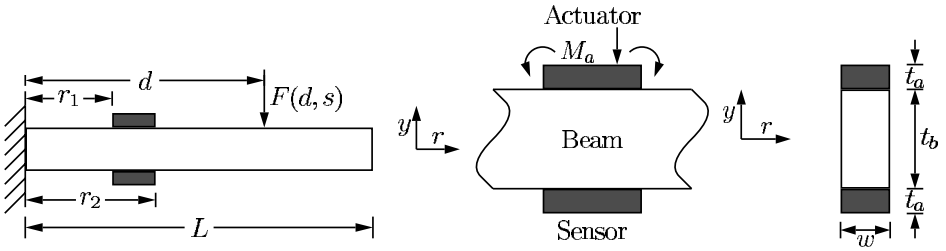

Figure 7. Piezoelectric laminate beam.

constrained to satisfy the following orthogonality property:

$$\int_0^L \phi_i(r)\phi_j(r)\rho A\,\mathrm{d}r = \rho AL^3\delta_{ij} \tag{9}$$

$$\int_0^L \phi_i''(r)\phi_j''(r)\rho A\,\mathrm{d}r = \rho AL^3\omega_i^2\delta_{ij} \tag{10}$$

where δ_{ij} is the Kronecker delta function. With this orthogonality and the boundary conditions, the mode shape is given by

$$\phi_i(r) = L\left(\cosh\lambda_i r - \cos\lambda_i r - \frac{\cos\lambda_i L + \cosh\lambda_i L}{\sin\lambda_i L + \sinh\lambda_i L} \times (\sinh\lambda_i r - \sin\lambda_i r)\right)$$

where λ_i are the roots of the following equation:

$$1 + \cos\lambda_i L \cosh\lambda_i L = 0.$$

Multiplying the Bernoulli–Euler equation (6) by $\phi_j(r)$ and integrating over $[0, L]$ we have

$$EI\int_0^L \sum_{i=0}^{\infty} q_i(t)\phi_i''''(r)\phi_j(r)\,\mathrm{d}r + \rho A\int_0^L \sum_{i=0}^{\infty}\ddot{q}_i(t)\phi_i(r)\phi_j(r)\,\mathrm{d}r = \int_0^L C_a\frac{\partial^2 v_a(x,t)}{\partial r^2}\phi_j(r)\,\mathrm{d}r. \tag{11}$$

The voltage $v_a(x, t)$ is constant in the range $[x_1, x_2]$, and the right-hand side of equation (11) can be written as

$$\int_0^L C_a\frac{\partial^2 v_a(x,t)}{\partial r^2}\phi_j(r)\,\mathrm{d}r = \int_0^L C_a[\delta'(x_1) - \delta'(x_2)]v_a(t)\phi_j(r)\,\mathrm{d}r = C_a[\phi_j'(x_1) - \phi_j'(x_2)]v_a(t). \tag{12}$$

Noting that $\phi_i''''(r) = \lambda^4\phi_i$, the ith mode equation can be written as

$$\rho AL^3\left(\ddot{q}_i(t) + \omega^2 q_i(t)\right) = C_a[\phi_i'(x_1) - \phi_i'(x_2)]v_a(t) \quad i = 1, \ldots, \infty. \tag{13}$$

The above modal equations (13) can be put together to give the following transfer function between the voltage applied to the piezoelectric patch, $V_a(r, t)$, and the displacement $y(r, t)$ [26, 23, 24]:

$$G_{vy}(s) \triangleq \frac{Y(r,s)}{V_a(s)} = \sum_{i=1}^{\infty}\frac{C_a\phi_i(r)[\phi_i'(r_1) - \phi_i'(r_2)]}{\rho AL^3\left(s^2 + \omega_i^2\right)} \tag{14}$$

where $C_a = \frac{1}{2}E_a d_{31} w(t_a + t_b)$, d_{31} is the electric charge constant of the film, E_a is Young's modulus of the film and t_a is the thickness of the piezo-patch. Also, the frequencies ω_i are related to λ_i by $\omega_i = \sqrt{\frac{EI}{\rho A}}\lambda_i^2$, where E, I, A, $V_a(r, t)$ and ρ represent Young's modulus, the moment of inertia, the cross-section area, the voltage across the actuating layer and the linear mass density of the beam, respectively.

Table 1. Parameters of the piezoelectric laminate beam.

Beam length, L	0.775 m
Beam width	0.05 m
Beam thickness, t_b	0.00589 m
Piezoceramic position, r_1	0.03 m
Piezoceramic position, r_2	0.10 m
Charge constant, d_{31}	-210×10^{-12} m v^{-1}
Voltage constant, g_{31}	-11.5×10^{-3} Vm N^{-1}
Coupling coefficient	0.340
Capacitance, C	32.9 nF
Piezoceramic width	0.025 m
Piezoceramic thickness t_a	1×10^{-3} m

Table 2. The first eight modes of the cantilever beam.

	ω_i (Hz)	
Mode	Experimental	Analytical
1	7.98	7.96
2	50.04	47.75
3	140.14	134.9
4	274.61	258.3
5	453.95	430.5
6	678.13	644.5
7	947.13	903
8	1261.0	1206

The parameters for the experimental beam at the University of Newcastle and the PIC151 piezoceramic parameters are given in table 1. The first eight values of ω_i for this beam are shown in table 2.

Equation (14) describes the elastic deflection of the entire flexible beam due to a voltage applied to the actuating piezoelectric layer. Our controller design is based on this particular model. The sensor voltage expression can be written as [27]

$$v_s(t) = C_s\sum_{i=1}^{\infty} q_i(t)(\phi_i'(r_2) - \phi_i'(r_1)).$$

Substituting the above expressions in the transfer functions defined earlier, we get

$$G_{fv}(s) \triangleq \frac{V_s(s)}{F(d,s)} = \sum_{i=1}^{\infty}\frac{C_s\phi_i(d)[\phi_i'(r_2) - \phi_i'(r_1)]}{\rho AL^3\left(s^2 + \omega_i^2\right)} \tag{15}$$

$$G_{vv}(s) \triangleq \frac{V_s(s)}{V_a(s)} = -\sum_{i=1}^{\infty} \frac{C_a C_s[\phi_i'(r_1) - \phi_i'(r_2)]^2}{\rho A L^3 \left(s^2 + \omega_i^2\right)} \quad (16)$$

and

$$G_{fy}(r, s) = \sum_{i=1}^{\infty} \frac{\phi_i(r)\phi_i(d)}{\rho A L^3 \left(s^2 + \omega_i^2\right)}. \quad (17)$$

In the next section we look at the closed-loop stability of the resonant controllers.

4. Closed-loop Stability

The passivity theorem [28] is used here to prove the stability of the closed-loop system. A linear system is said to be passive if the phase of its frequency response is within $\pm 90^\circ$, i.e. it stays in the first and the fourth quadrant. The passivity theorem states that a feedback interconnection of two passive systems is passive. In the following we show that the closed-loop system can be written as an interconnection of two passive systems.

Theorem 1. *The closed-loop system*

$$V_s(s) = \frac{G_{vv}(s)V_i(s)}{1 + \sum_{i=1}^{N} sG_{vv}(s)\tilde{A}_i(s)}$$

with

$$\tilde{A}_i(s) = -k_{ai}\frac{C_i(R_i + L_i s)}{L_i C_i s^2 + R_i C_i s + 1}$$

is stable for all $L_i > 0$, $R_i > 0$, $C_i > 0$ *and* $k_{ai} > 0$.

From equation (16) we have

$$-sG_{vv}(s) = \sum_{i=1}^{\infty} \frac{sC_a C_s[\phi_i'(r_1) - \phi_i'(r_2)]^2}{\rho A L^3 \left(s^2 + \omega_i^2\right)}.$$

It can be easily verified that $\Re\left\{\frac{j\omega}{-\omega^2+\omega_i^2}\right\} \geqslant 0, \forall\omega \in [-\infty, \infty]$, that is $\frac{s}{s^2+\omega_i^2}$ is passive. Further defining,

$$c_i \triangleq \frac{C_a C_s[\phi_i'(r_1) - \phi_i'(r_2)]^2}{\rho A L^3}$$

$-sG_{vv}(s)$ can be seen as a positively weighted ($c_i > 0$) sum of passive transfer functions. This implies that $-sG_{vv}(s)$ is passive [28]. Similarly it can be seen that $\tilde{A}_i(s)$ is strictly passive ($\tilde{A}_i(j\omega) + \tilde{A}_i(-j\omega) \geqslant 0\ \forall\omega$). Again $\tilde{A}(s)$ is a sum of positively weighted transfer functions, hence the strict passivity of $\tilde{A}(s)$. The stability of the closed-loop system is due to the passivity theorem [28] which states that a negative feedback interconnection of a passive system and a strictly passive system is stable.

Remarks

1. With the above definition $\tilde{A}_i(s) = \frac{A_i(s)}{s}$, where $A_i(s)$ are the resonant controllers given in equation (2). Theorem 1 proves the stability of the closed-loop systems considered in this paper. The theoretical gain margin of these controllers is infinity.
2. The above discussion implies that the phase of $G_{vv}(s)$ is always between 0° and 180°, implying the well-known pole-zero interlacing property of the colocated transfer functions.

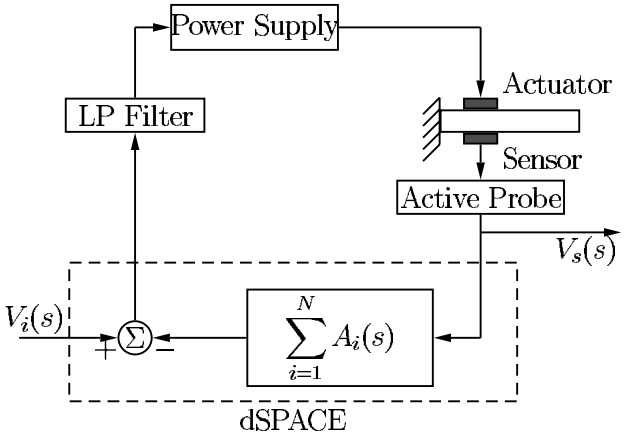

Figure 8. Experimental beam.

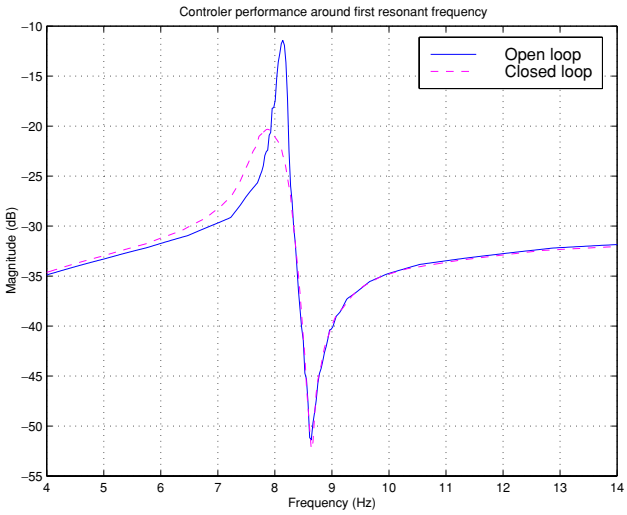

Figure 9. Experimental frequency response for the first mode.

5. Experimental verification

The experimental set-up at the University of Newcastle is shown in figure 8. A cantilever beam with two piezoelectric patches is used to demonstrate the method. The parameters for the beam are given in table 1. A lowpass filter with a cut-off at 300 Hz is used to filter out the effect of discretized output from the digital controller. A Tektronix active probe was used to sample the sensor voltage to avoid loading the sensor. A ds1102 dSPACE board is used to implement the digital controller with a 2 kHz sampling frequency. A HP spectrum analyser was used to obtain frequency response between $V_s(s)$ and $V_i(s)$ as shown in figure 8.

Experiments were performed to damp the first, second and third modes, both individually and jointly. The resonant controller for the first mode $A_1(s)$ can be built with $\omega_1 = 7.98$ Hz, $R_1 = 2.5\,\text{k}\Omega$, $C_1 = 1\,\mu$F and $L_1 = 39.716$ H. Figure 9 shows the open-loop and closed-loop frequency responses of the system. The sinusoidal response (7.98 Hz) of the open-loop and closed-loop systems is shown in figure 10.

The responses with the resonant controller ($\omega_2 = 49.9$ Hz, $R_2 = 250\,\Omega$, $C_2 = 1\,\mu$F and $L_2 = 10.994$ H), to control the second mode, are shown in figures 11 and 12. These figures

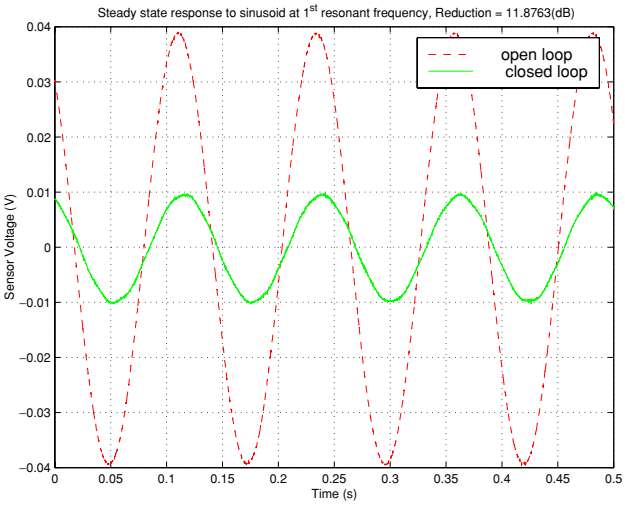

Figure 10. Experimental sinusoidal response for the first mode.

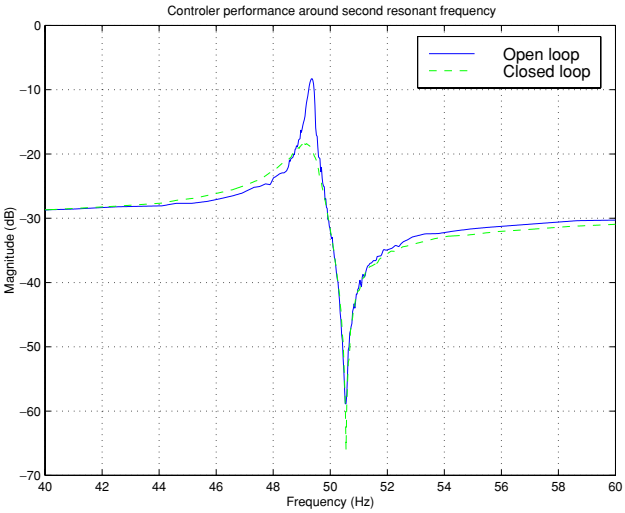

Figure 11. Experimental frequency response for the second mode.

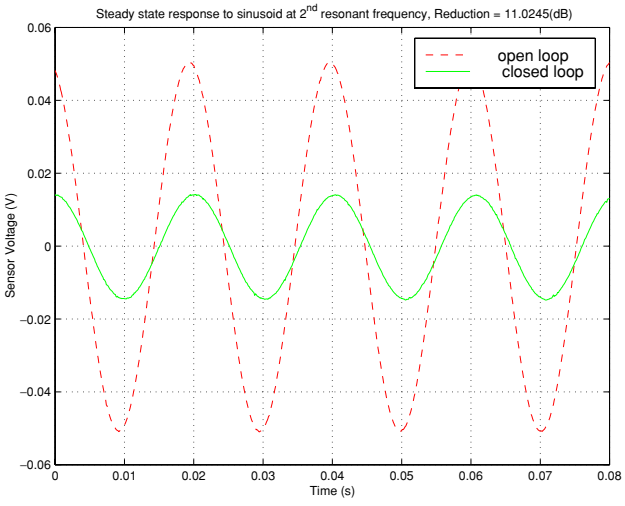

Figure 12. Experimental sinusoidal response for the second mode.

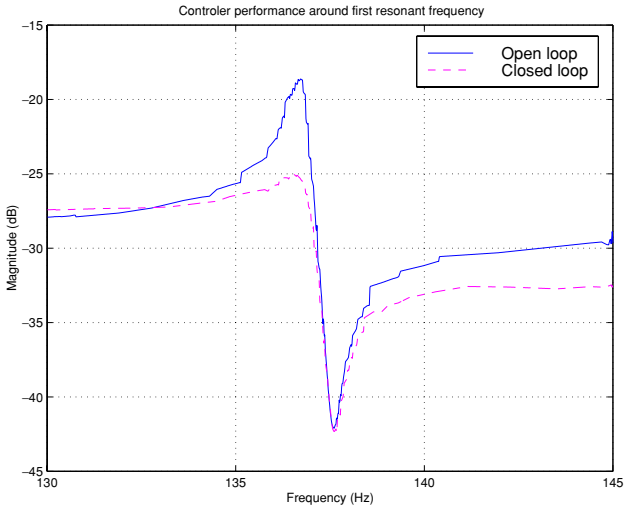

Figure 13. Experimental frequency response for the third mode.

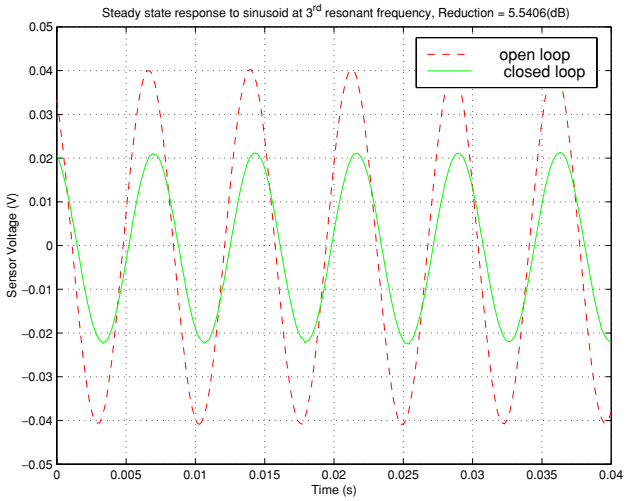

Figure 14. Experimental sinusoidal response for the third mode.

clearly demonstrate the improvement due to the resonant controller.

The third mode controller $A_3(s)$ for the resonant frequency $\omega_3 = 135$ Hz needs $R_3 = 130\,\Omega$, $C_3 = 1\,\mu$F and $L_3 = 1.3899$ H. Figures 13 and 14 show the frequency response and the sinusoidal response for the open-loop and closed-loop systems, respectively. Again the improvement in the response is obvious.

Note that the resonant peak in figure 13 has almost disappeared.

5.1. All three mode controllers

All three modes can be damped simultaneously using one sensor–actuator pair and three parallel combinations of resonant mode controllers. The frequency response of such a system is shown in figure 15. Figure 16 shows the frequency response for the entire frequency range of interest. The robustness of the method is clearly demonstrated from these figures.

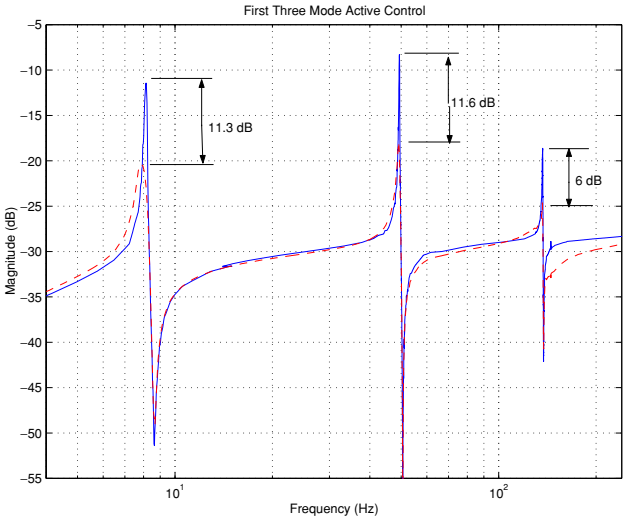

Figure 15. Experimental frequency response for the first three modes: solid, open-loop; dashed, closed-loop.

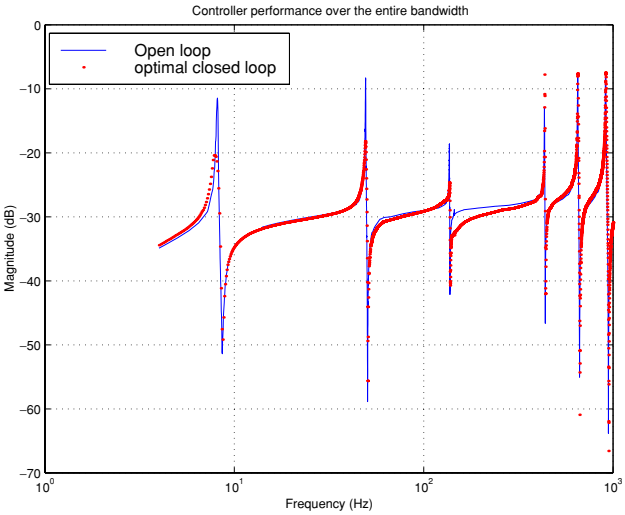

Figure 16. Experimental frequency response for the first six modes.

6. Conclusions

The experiments have shown the effectiveness of the proposed resonant controllers, both in their robustness and multi-modal control of smart structures. The structure of these controllers is simple and they can be implemented very easily using passive circuit elements and two op-amps. These controllers can be effectively used to damp other distributed parameter systems, e.g. active control of acoustic noise. In conclusion, in this paper we present a simple and yet effective method to damp oscillations in distributed parameter systems such as smart structures.

References

[1] Fukuda T, Takawa T and Nakashima K 2000 Optimum vibration control of CFRP sandwich beam using electro-rheological fluids and piezoceramic actuators *Smart Mater. Struct.* **9** 121

[2] Guigou C and Fuller C R 1997 Foam-pvdf smart skin for aircraft interior sound control *Proc. SPIE Smart Structures and Materials (San Diego, CA, 4–6 March)* vol 3044, ed Janet M Slater, pp 68–78

[3] Tappert P M, Mercadal M and von Flotow A H 1997 Evaluation of actuation schemes used for acoustic attenuation of vibrating surfaces *Proc. SPIE Smart Structures and Materials (San Diego, CA, 4–6 March)* vol 3044, ed Janet M Slater, pp 79–86

[4] Diana G, Cheli F, Coppola M and Conrad D C 1997 Active control of vibrations of a metal panel by means of piezoelectric actuators and sensors *Proc. SPIE Smart Structures and Materials (San Diego, CA, 4–6 March)* vol 3044, ed Janet M Slater, pp 327–41

[5] Pota H R, Moheimani S O R and Smith M 1999 Resonant controllers for flexible structures *Proc. IEEE International 38th Conf. on Decision and Control (Phoenix AZ, 7–10 Dec.)* (Piscataway, NJ: IEEE) pp 631–6

[6] Pota H R and Kelkar A G 2001 Modelling and control of acoustic ducts *ASME J. Vib. Acoust.* **123** 2

[7] Nye T W, Manning R A and Qassim K 1999 Performance of active vibration control technology: the actex flight experiments *Smart Mater. Struct.* **8** 767

[8] Bronowick A J, Abhyankar N S and Griffin S F 1999 Active vibration control of large optical space structures *Smart Mater. Struct.* **8** 740

[9] Fuller C R, Elliott S J and Nelson P A 1996 *Active Control of Vibration* (New York: Academic)

[10] Inman D J 1989 *Vibration with Control, Measurement, and Stability* (Englewood Cliffs, NJ: Prentice-Hall)

[11] Meirovitch L 1986 *Elements of Vibration Analysis* 2nd edn (Sydney: McGraw-Hill)

[12] Gevarter W 1970 Basic relations for control of flexible vehicles *AIAA J.* **8** 666

[13] Balas M J 1978 Feedback control of flexible structures *IEEE Trans. Autom. Control* **23** 673

[14] Goh C J and Caughey T K 1985 On the stability problem caused by finite actuator dynamics in the collocated control of large space structure *Int. J. Control* **41** 787

[15] Fanson J L and Caughey T K 1990 Positive position feedback control for large space structures *AIAA J.* **28** 717

[16] Friswell M I and Inman D J 1999 The relationship between positive position feedback and output feedback controllers *Smart Mater. Struct.* **8** 285

[17] Junkins J L and Kim Y 1993 *Introduction to Dynamics and Control of Flexible Structures* (Washington, DC: AIAA)

[18] Moheimani S O R, Pota H R and Petersen I R 1999 Spatial balanced model reduction for flexible structrues *Automatica* **35** 269

[19] Moheimani S O R, Petersen I R and Pota H R 1999 Broadband disturbance attenuation over an entire beam *J. Sound Vib.* **227** 807

[20] Petersen I R and Pota H R 2001 Minimax LQG optimal control of a flexible beam *Control Eng. Pract.* at press

[21] Hagood N W, Chung W H and von Flotow A 1990 Modelling of piezoelectric actuator dynamics for active structural control *J. Intell. Mater. Syst. Struct.* **21** 327

[22] Wang K W 1995 Structural vibration suppression via parametric control actions—piezoelectric materials with real-time semi-active networks *Wave Motion, Intelligent Structures and Nonlinear Mechanics* ed A Guran and D J Inman (Singapore: World Scientific) pp 112–34

[23] Alberts T E and Colvin J A 1991 Observations on the nature of transfer functions for control of piezoelectric laminates *J. Intell. Mater. Syst. Struct.* **2** 528

[24] Pota H R and Alberts T E 1995 Multivariable transfer functions for a slewing piezoelectric laminate beam *Trans. ASME, J. Dyn. Syst. Meas. Control* **117** 352

[25] Fraser A R and Daniel R W 1991 *Perturbation Techniques for Flexible Manipulators* (Dordrecht, MA: Kluwer)

[26] Moheimani S O R, Pota H R and Petersen I R 1998 Spatial control for active vibration control of piezoelectric

laminates *Proc. Conf. Decision and Control (Tampa, FL, 16–18 Dec.)* (Piscataway, NJ: IEEE) pp 4308–12

[27] Moheimani S O R, Pota H R and Petersen I R 1998 Active control of a piezo-electric laminate cantilevered beam *Proc. Int. Symp. on Intelligent Robotic Systems (Bangalore, India, Jan.)* ed M Vidyasagar (New Delhi: Tata McGraw-Hill) pp 505–12

[28] Desoer C A and Vidyasagar M 1975 *Feedback Systems: Input-Output Properties* (New York: Academic)